Bioorganic & Medicinal Chemistry 21 (2013) 1992–2000

Contents lists available at SciVerse ScienceDirect

Bioorganic & Medicinal Chemistry

journal homepage: www.elsevier.com/locate/bmc

Novel pseudopeptides incorporating a benzodiazepine-based turn mimetic—targeting *Mycobacterium tuberculosis* ribonucleotide reductase

Johanna Nurbo [a], Daniel J. Ericsson [b], Ulrika Rosenström [a], Daniel Muthas [a], Anna M. Jansson [b], Gunnar Lindeberg [a], Torsten Unge [b], Anders Karlén [a,*]

[a] Department of Medicinal Chemistry, Organic Pharmaceutical Chemistry, BMC, Uppsala University, Box 574, SE-751 23 Uppsala, Sweden
[b] Department of Cell and Molecular Biology, Structural Biology, BMC, Uppsala University, Box 596, SE-751 24 Uppsala, Sweden

ARTICLE INFO

Article history:
Received 5 October 2012
Revised 8 January 2013
Accepted 11 January 2013
Available online 18 January 2013

Keywords:
Mycobacterium tuberculosis
Ribonucleotide reductase
Peptide inhibitor
Pseudopeptide

ABSTRACT

Peptides mimicking the C-terminus of the small subunit (R2) of *Mycobacterium tuberculosis* ribonucleotide reductase (RNR) can compete for binding to the large subunit (R1) and thus inhibit RNR activity. Moreover, it has been suggested that the binding of the R2 C-terminus is very similar in *M. tuberculosis* and *Salmonella typhimurium*. Based on modeling studies of a crystal structure of the holocomplex of the *S. typhimurium* enzyme, a benzodiazepine-based turn mimetic was identified and a set of novel compounds incorporating the benzodiazepine scaffold was synthesized. The compounds were evaluated in a competitive fluorescence polarization assay and in an RNR activity assay. These studies revealed that the compounds incorporating the benzodiazepine scaffold have the ability to compete for the *M. tuberculosis* R2 binding site with low-micromolar affinity.

1. Introduction

Tuberculosis is an infection that mainly affects the lungs and is caused by the pathogen *Mycobacterium tuberculosis*. In 2010, the World Health Organization estimated 8.8 million new cases of tuberculosis worldwide.[1] Since the disease remains a global health crisis with an alarming rise of multi-drug resistant[2] and extensively drug resistant[2,3] bacterial strains, the need for new antitubercular therapeutics is very urgent.

M. tuberculosis ribonucleotide reductase (RNR) has been identified as a potential drug target.[4,5] RNR is responsible for the reduction of ribonucleotides to the corresponding deoxyribonucleotides and the bioactive enzyme is composed of two larger (R1) and two smaller subunits (R2).[6] Association of the subunits is essential for catalytic activity because the substrate binding site is located on R1, while R2 harbors a radical involved in the reduction. The C-terminus of R2 is crucial for this association and small peptides corresponding to the C-terminal sequence can compete for binding to R1 and thus inhibit the enzyme.[7,8] In *M. tuberculosis*, R1 and R2 are encoded by the genes *nrdE* (Rv3051c) and *nrdF2* (Rv3048c).[4,9] These genes have been identified as essential for optimal bacterial growth in a transposon site hybridization study.[10] It has also been shown by gene knockout studies, that the combination of these two genes is required for bacterial growth.[4] In addition, Mowa et al.[5] have suggested that the product of these genes, the NrdEF2 enzyme, provides the RNR activity required by the bacteria for DNA synthesis and repair at every stage of infection.

We have previously reported on the evaluation of a set of N-acetylated peptide inhibitors based on the C-terminal end of the *M. tuberculosis* RNR R2 subunit.[8] Starting from the heptapeptide Ac-Glu1-Asp2-Asp3-Asp4-Trp5-Asp6-Phe7 (**1**) we could show that Trp5 and Phe7 are important for inhibition of enzyme activity. Furthermore, our study indicated that there is room for larger side-chains, as compared to Trp, in position 5. This was also supported by inspection of the X-ray structure of *Salmonella typhimurium* RNR.[11] Interestingly, studies on mammalian RNR have revealed that Fmoc-protected peptides can work as inhibitors of the enzyme.[12,13] Encouraged by these results, we could also show that an N-terminal Fmoc group could be advantageous in potential R2 C-terminal derived peptide inhibitors of *M. tuberculosis* RNR.[14]

Incorporation of secondary structure mimetics is an alternative strategy to transform biologically active peptides into nonpeptides. This approach has already been employed in the search for inhibitors of mammalian RNR.[15,16] By studying the *S. typhimurium* RNR holocomplex, we were inspired to explore the use of turn mimetics in our development of less peptidic inhibitors targeting *M. tuberculosis* RNR. There are several successful examples of benzodiazepine-based scaffolds as turn mimetics.[17–20] In this Letter, we report on the design and synthesis of novel pseudopeptides

* Corresponding author. Tel.: +46 18 471 4293; fax: +46 18 471 4474
E-mail address: anders.karlen@orgfarm.uu.se (A. Karlén).

0968-0896/$ - see front matter © 2013 Elsevier Ltd. All rights reserved.
http://dx.doi.org/10.1016/j.bmc.2013.01.020

comprising a benzodiazepine turn scaffold. The target compounds are evaluated, with respect to binding affinity for the *M. tuberculosis* R1 subunit, using a competitive fluorescence polarization (FP) assay. Selected compounds were also evaluated using an activity assay where the reduction of CDP is monitored.

2. Results and discussion

2.1. Molecular modeling

In 2006, Uppsten et al. reported the 4 Å structure of the R1/R2 complex from *S. typhimurium* (PDB ID: 2BQ1) and it was suggested that the binding of the last eight residues of the R2 C-terminus to R1 is very similar in *S. typhimurium* and *M. tuberculosis*.[11] Unfortunately only the side chains of Thr, Trp and Phe in the R2 C-terminal peptide (Thr-Glu-Asp-Glu-Asp-Trp-Asn-Phe) of the *S. typhimurium* R1/R2 complex could be identified from the obtained electron density and the remaining amino acids were built as Ala in the reported structure. Furthermore, only the carbon of the R2 C-terminal carboxyl group was present in the PDB structure. Nevertheless this was an excellent starting point for our further peptidomimetic design efforts, since we had previously shown that both Trp5 and Phe7 in **1** are important for inhibiting *M. tuberculosis* RNR. We thus decided to investigate if it was possible to substitute part of the C-terminal region of **1** with a turn mimetic. Overlay with different turn scaffolds previously investigated by our group, revealed that a benzodiazepine based scaffold, originally developed as a γ-turn mimic, as a potential mimetic.[21] In the comparison we used the model compounds **1m** and **11m** shown in Figure 1A and B, respectively. Model compound **1m** represents the C-terminal fragment of peptide **1** and **11m** the corresponding fragment with the benzodiazepine scaffold incorporated. Based on an atom to atom comparison of the back-bones of **1m** to **11m** there is an excellent fit to the benzodiazepine structure. To investigate if the model compound **11m** also can adopt a similar overall 3D-shape as the C-terminal fragment **1m**, including the orientation of the Trp and Phe side chains, a conformational analysis of **11m** was performed.

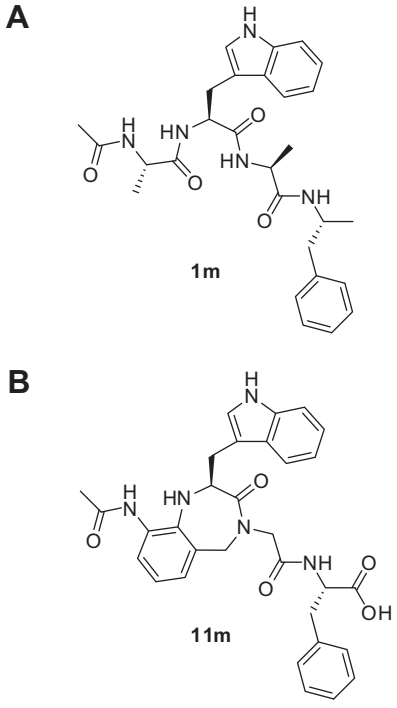

Figure 1. Structures used in molecular modeling and conformational analysis. (A) C-terminal fragment of R2, derived from the crystal structure of *S. typhimurium* RNR (note that the oxygens in the C-terminal carboxyl group are lacking in the PDB structure). (B) Model compound, incorporating the benzodiazepine scaffold.

The 3D-structure of the peptide fragment **1m**, based on the crystal structure of *S. typhimurium* RNR, is shown in Figure 2A. The conformational analysis of model compound **11m** was performed using the OPLS_2005 force field[22] and the general Born Solvent Accessible (GB/SA) water solvation model[23] in Macromodel.[24] The number of conformations within 5 kcal/mol of the global energy minimum found for **11m** was 872. These conformations were then compared to model compound **1m** (Fig. 2A) by using 3D-shape screening in phase 3.1 in the Maestro modeling environment. In this approach, the phase_shape program searches for the conformations of **11m** that are most similar in 3D shape to **1m**. The conformer and alignment that gave the highest similarity is shown in Figure 2B. In general the overlap between these two structures is very good as seen for the C-terminal carbonyl carbon and the Phe and Trp side chains, although the direction of the N-terminal acetyl fragments are oriented somewhat differently. Encouragingly, when the R1 protein is included it can be seen that **11m** also fits nicely in the cavity (Fig. 2C). The Phe side chain seems to be making contact with Arg685 in R1, although it should be noted that the density for the

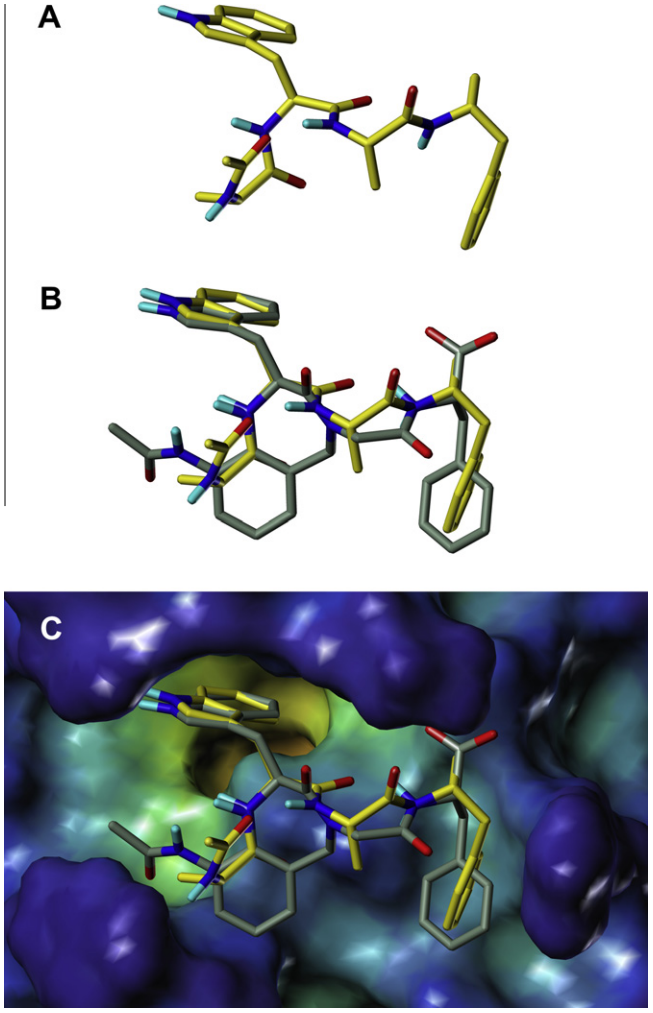

Figure 2. Comparison of the C-terminal fragment of the *S. typhimurium* R2 (**1m**) and the model compound **11m** incorporating the benzodiazepine scaffold. (A) Conformation of peptide fragment **1m**, in the crystal structure of *S. typhimurium* RNR. (B) Shape aligned conformer of **11m** that gave the highest similarity. (C) Same as in B but with the surface of the protein included (Connolly surface with color coding according to cavity-depth).

Table 1
Structures, dissociation constants and inhibitory potency values of benzodiazepine-based compounds

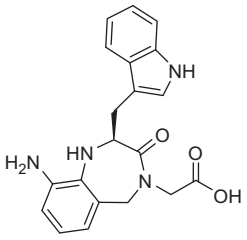

I

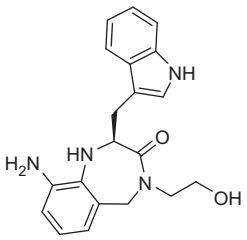

II

Compound	Sequence	K_{D2} ± SD[a] (μM)	IC_{50} ± SD[b] (μM)
1	Ac-Glu-Asp-Asp-Asp-Trp-Asp-Phe	8.3 ± 0.3	20 ± 10
11	Ac-Glu-Asp-Asp-**I**-Phe	81 ± 13	
12	Ac-Glu-Asp-Asp-Asp-**I**-Phe	27 ± 2	64 ± 9
13	Ac-Asp-**I**-Phe	>150	
14	Fmoc-Asp-**I**-Phe	1.6 ± 0.2	
15	Fmoc-**I**	8.1 ± 0.1	24 ± 2
17	Fmoc-**II**	26 ± 1	171 ± 67

[a] K_{D2} is the dissociation constant of the interaction between R1 and compound.
[b] IC_{50} is the inhibitory capacity where the reduction of CDP is monitored.

Arg side chain is not well defined in the complex. The side chain of Trp can be seen pointing down into the hydrophobic cleft.

We thus decided to incorporate this scaffold into peptide **1** to give pseudopeptide **11** (Table 1). Because of synthetic reasons, the side chain corresponding to Asp6 was omitted in the turn scaffold. However, this should not have a detrimental effect on the activity since our earlier studies have shown that exclusion of the carboxylic acid functionality in this position only results in a two-fold drop in potency.[8] Since the direction of the N-terminal amino acid entering the turn mimetic in **11m** was slightly different as compared to **1m** we decided to also incorporate the longer fragment Glu-Asp-Asp-Asp to give pseudopeptide **12**. We also decided to introduce the benzodiazepine scaffold in shorter analogues of **1** with either an *N*-acetyl or an Fmoc protecting group (compound **13** and **14**, respectively). Compound **14** was prepared because we recently showed that the Fmoc group had a beneficial effect on binding. The corresponding *N*-acetyl analogue (**13**) was prepared as a reference compound. Furthermore, we have previously shown that Fmoc-Trp has a binding affinity comparable to that of peptide **1**,[14] and therefore also prepared compound **15**. In addition, the alcohol analogue **17** was generated.

2.2. Chemistry

The benzodiazepine based scaffold investigated in this study allows introduction of numerous different amino acid equivalents and can be coupled into a peptide sequence using standard solid phase peptide synthesis (SPPS) methodology. Hence, the tryptophan-based benzodiazepine turn mimetic **10** was synthesized in solution followed by incorporation using standard SPPS methodology to give the pseudopeptides **11**–**14**. Scaffold **10** was generated essentially following the procedure for the preparation of turn mimetics described by Rosenström et al.[21] and the synthetic route is outlined in Scheme 1. First, the aldehyde **3**[21] was synthesized from 2-chloro-3-nitrobenzoic acid (**2**) by reduction to the alcohol and a subsequent Swern oxidation. Preparation of the protected alcohol **4** started with a reductive amination of **3** with 2-aminoethanol. The generated alcohol was then protected using *tert*-butyldimethylchlorosilane (TBDMSCl). In the following step, **4** was coupled with Fmoc-L-Trp-OH using *N*-[(dimethylamino)-1*H*-1,2,3-triazolo-[4,5-*b*]pyridine-1-yl-methylene]-*N*-methylmethanaminium hexafluorophosphate *N*-oxide (HATU) as activating reagent in the presence of *N*,*N*-diisopropylethylamine (DIEA). Fmoc-deprotection was achieved by treatment with 1,8-diazabicyclo[5.4.0]undec-7-ene (DBU) to give the free amine **5**. The subsequent intramolecular nucleophilic aromatic substitution proceeded in Et_3N and dimethylsulfoxide (DMSO) at 100 °C to deliver the cyclized product **6**. To generate the benzodiazepine **7**, the tryptophan indole was protected using Boc-anhydride and *N*,*N*-dimethyl-4-aminopyridine (DMAP). Direct incorporation of Fmoc-L-Trp(Boc)-OH was not compatible with the cyclization reaction protocol. Under these high-temperature conditions the Boc-protecting group was cleaved off to some extent. The alcohol **8** was obtained by cleavage of the TBDMS-protecting group by tetrabutylammonium fluoride (TBAF). Then, the carboxylic acid **9** was synthesized in a two step reaction starting with a Swern oxidation to the aldehyde, followed by additional oxidation using sodium chlorite. Finally, reduction of the nitro group of **9** was performed by catalytic hydrogenation and the resulting amine was protected with FmocCl to give the scaffold **10**.

Pseudopeptides **11**–**14** were prepared manually from *H*-L-Phe-2-chlorotrityl resin. The coupling of scaffold **10** to the solid phase was performed in *N*,*N*-dimethylformamide (DMF), using (benzotriazol-1-yl-oxy)tripyrrolidinophosphonium hexafluorophosphate (PyBOP) in the presence of DIEA. For introduction of the additional amino acids, the same conditions were used. After completion of the sequences, the terminal amino group of pseudopeptide **11**–**13** was acetylated by acetic anhydride whereas the Fmoc group of **14** was retained. The crude pseudopeptides were purified by preparative RP-HPLC and the overall yields ranged from 14% to 45%.

Also, the deprotected turn mimetic **15** was generated by treatment of **10** with TFA (Scheme 2). Furthermore, the corresponding alcohol **17** was produced by catalytic hydrogenation of **7** followed by coupling with FmocCl to give **16** (Scheme 3). The Boc-group of the indole and the TBDMS-group on the alcohol were both removed by TFA to deliver **17**.

2.3. Biochemical evaluation

Target compounds **11**–**15**, **17** and reference compound **1** were tested in an FP assay. In the assay the compounds competed with a fluorescent probe, incorporating the R2 C-terminal sequence, for binding to R1.[14] The compounds that showed the best binding

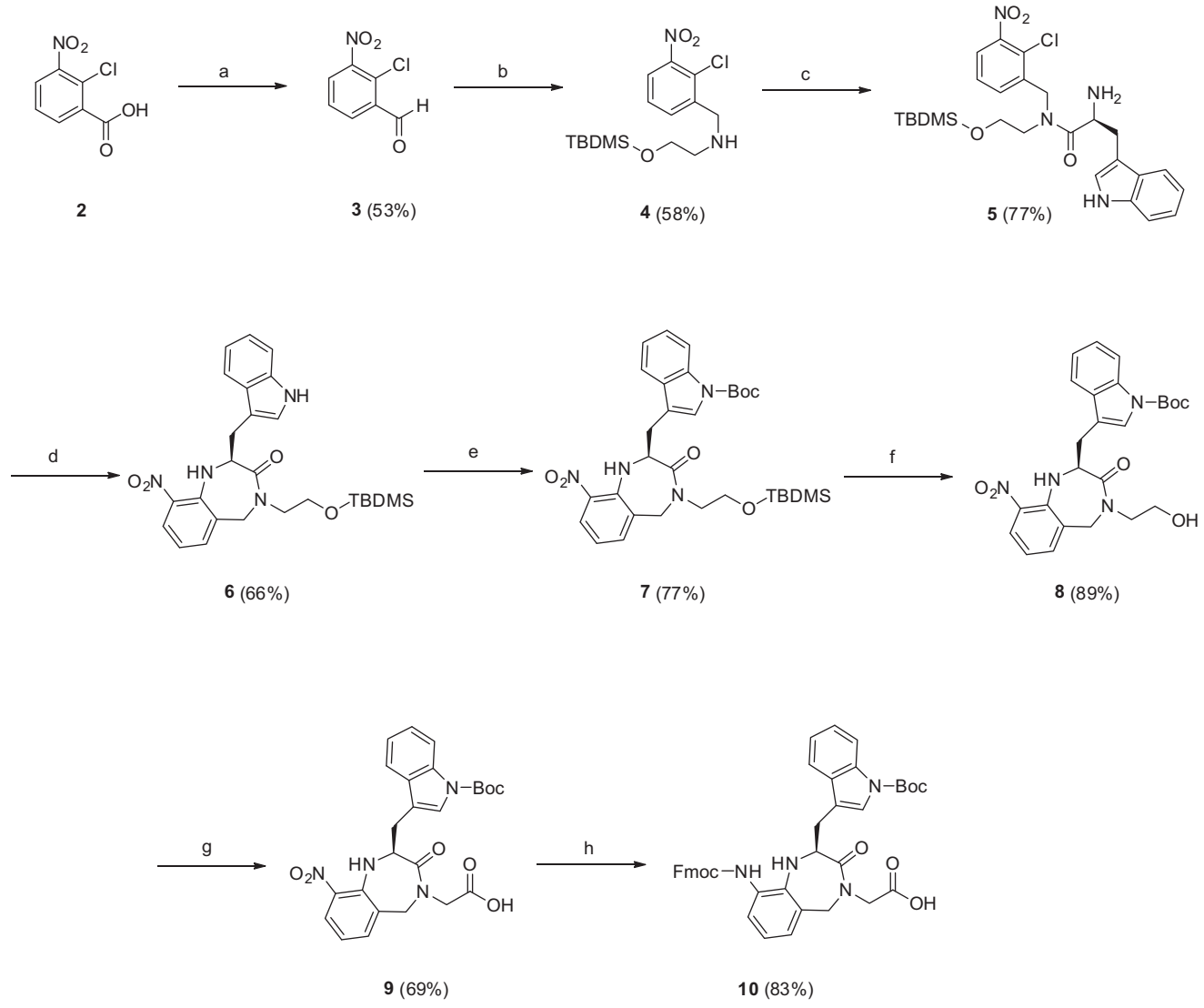

Scheme 1. Reagents and conditions: (a) (i) $NaBH_4$, $BF_3{\cdot}Et_2O$, THF, (ii) oxalyl chloride, DMSO, Et_3N, DCM; (b) (i) 2-aminoethanol, HOAc, $NaCNBH_3$, MeOH, (ii) TBDMSCl, DBU, THF; (c) (i) Fmoc-L-Trp-OH, HATU, DIEA, DCM, (ii) DBU, THF; (d) Et_3N, DMSO; (e) Boc_2O, DMAP, MeCN; (f) TBAF, THF; (g) (i) oxalyl chloride, DMSO, Et_3N, DCM, (ii) $NaClO_2$, NaH_2PO_4, cyclohexene, *t*-BuOH, H_2O; (h) (i) H_2, Pd/C, MeOH, (ii) FmocCl, Na_2CO_3 (aq), 1,4-dioxane.

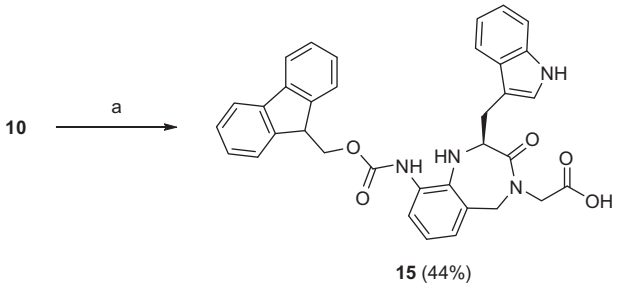

Scheme 2. Reagents and conditions: (a) TFA, DCM.

in the FP assay and for which material was available were also evaluated for their inhibitory capacity using the [^{3}H]CDP assay where the reduction of CDP is monitored.[8] Structures, dissociation constants (K_{D2} values) and inhibitory potency values (IC_{50}) are presented in Table 1

Incorporation of the benzodiazepine-based scaffold into the sequence of peptide **1** gave pseudopeptide **11** with a K_{D2} value of 81 μM. Introduction of the additional Asp residue of **12** resulted in improved binding properties (K_{D2} = 27 μM). Interestingly, incorporation of the benzodiazepine turn mimetic in **1** gave a 10-fold drop in potency for **11** but only a three-fold drop in potency for **12**. That **12** has a lower K_{D2} value than **11** could be a consequence of an overall better fit of the pseudopeptide **12** to the binding site. This could be due to extra interactions of the additional amino acid of **12**, improving the binding affinity as compared to **11**. Alternatively, there is a poorer match between the native peptide and the turn mimetic than suggested by modeling and the extra Asp residue in **12** is needed to place the amino acids Glu-Asp-Asp in a more favorable position for binding.

The N-acetylated pseudopeptide **13** (K_{D2} = >150 μM) exhibited a very poor binding affinity. Most interestingly, when an Fmoc-protecting group is introduced in the same sequence (**14**), the K_{D2} value is improved to 1.6 μM. The poor binding affinity of **13** is supported by the SAR obtained from the series of *N*-acetyl truncated peptides that showed that at least a hexapeptide is needed for inhibition at micromolar concentrations.[8] Similarly, the beneficial effect of introducing an Fmoc group in short peptides is seen for compound **14**, which has the best binding affinity in this series.

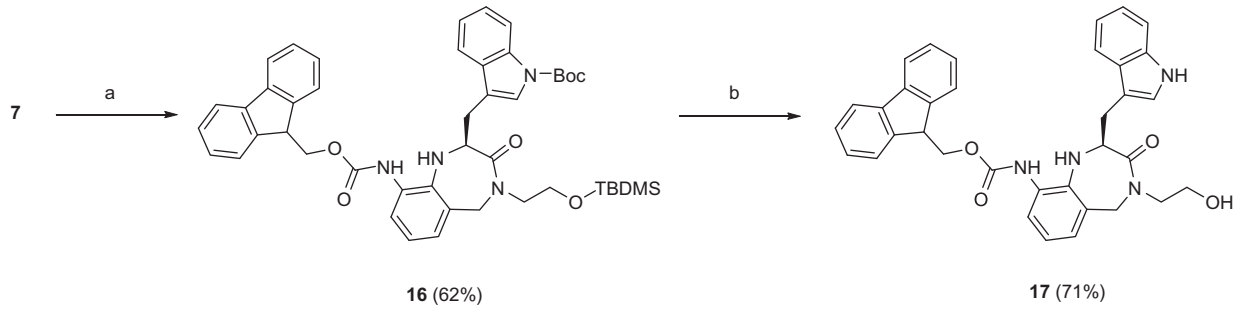

Scheme 3. Reagents and conditions: (a) (i) H_2, Pd/C, EtOH, (ii) FmocCl, Na_2CO_3 (aq), 1,4-dioxane; (b) TFA, DCM.

Evaluation of compound **15** (K_{D2} = 8.1 μM) revealed that the Fmoc-protected benzodiazepine scaffold, lacking the C-terminal Phe residue, had a K_{D2} value comparable to peptide **1**. Substitution of the C-terminal carboxylic acid functionality with the corresponding hydroxylic group, as in compound **17** (K_{D2} = 26 μM), only reduces the ability to compete for the R2 binding site by a factor of three as compared to **15**. However, without an X-ray structure it is very difficult to speculate how compound **15** and **17** bind in the protein cavity.

Finally, we decided to study the best compounds in Table 1 (for which material was available) using the activity assay measuring the reduction of tritium labeled cytidine diphosphate. The IC_{50} of the reference compound **1** was seven times better in the present study as compared to our previously reported value.[8] This most likely reflects the slightly modified assay conditions were the experimental procedure has been optimized. However, it was pleasing to learn that the compounds that had affinity for *M. tuberculosis* R1 also were active in the activity assay. Furthermore, there was a reasonable correlation between the K_{D2} and IC_{50} values.

3. Conclusions

Based on modeling studies, a benzodiazepine-based turn mimetic has been identified, synthesized and incorporated into the acetylated heptapeptide corresponding to the R2 C-terminus of *M. tuberculosis* RNR. The benzodiazepine scaffold successfully replaced amino acids of the original sequence and was thus able to mimic the starting peptide. Smaller benzodiazepine analogues were also prepared and showed binding affinity to R1 comparable to the original heptapeptide. The activities of these compounds were also confirmed in an activity assay. Benzodiazepines are considered as privileged structures and these compounds should therefore serve as excellent starting points for the development of potent nonpeptide inhibitors of *M. tuberculosis* RNR.

4. Experimental section

4.1. Chemistry: general

Reagents and solvents were obtained commercially and used without further purification. TLC was performed using aluminium sheets precoated with silica gel 60 F_{254} (Merck) with visualization of spots using UV-detection and/or ninhydrin treatment followed by heating. Column chromatography was performed using silica gel 60 (40–63 μm) (Merck). LC–MS was carried out on a Gilson–Finnigan AQA system in ESI mode using a Chromolith SpeedROD RP-18e 4.6 × 50 mm column (Merck) and a CH_3CN/H_2O linear gradient with 0.05% HCOOH. Preparative RP-HPLC was done using a Zorbax SB-C8, 5 μm, 21.2 × 150 mm column. The purity of the inhibitors was determined by analytical RP-HPLC in the following systems (UV detection at 220 nm): column 1 (ACE 5 C18, 50 × 4.6 mm, H_2O/MeCN gradient with 25 mM NH_4OAc, pH 6.3) and column 2 (Thermo Hypersil C4, 50 × 4.6 mm, 5 μm, H_2O/MeCN gradient with 0.1% TFA). Optical rotation was measured on a Perkin–Elmer model 241 polarimeter. NMR spectra were recorded on a Varian Mercury plus spectrometer (^1H at 399.8 MHz, ^{13}C at 100.5 MHz) at ambient temperature unless otherwise stated. Chemical shifts are reported as δ values in ppm and are indirectly referenced to TMS via the solvent signal (^1H: $CHCl_3$ δ 7.26, CHD_2OD δ 3.31, DMSO-d_5 δ 2.50; ^{13}C: $CDCl_3$ δ 77.2). Exact molecular masses were determined on a Micromass Q-Tof2 mass spectrometer equipped with an electrospray ion source. Elemental analyses were performed by Analytische Laboratorien, Lindlar, Germany.

4.1.1. 2-Chloro-3-nitrobenzaldehyde (3)

Compound **3** was synthesized as previously reported[21] starting from 2-chloro-3-nitrobenzoic acid (10 g, 50 mmol) to give **3** (4.9 g, 53%) as beige solid.

4.1.2. 2-(*tert*-Butyldimethylsilyloxy)-*N*-(2-chloro-3-nitrobenzyl)ethanamine (4)

To a solution of **3** (4.7 g, 25 mmol) in MeOH (250 mL) was added 2-aminoethanol (7.6 mL, 127 mmol) and HOAc (2.3 mL, 41 mmol). After 10 min $NaCNBH_3$ (1.75 g, 28 mmol) was added and the reaction mixture was refluxed for 2.5 h. The mixture was cooled to room temperature and was acidified to pH 1 by addition of 2.0 M aqueous HCl. The residue was partly evaporated and was extracted with diethyl ether. The organic layer was washed with H_2O and brine, dried with $MgSO_4$ and was concentrated by rotary evaporation to give 2-(2-chloro-3-nitro-benzylamino)ethanol[21] as a solid. The unprotected alcohol in MeCN (120 mL) was cooled in an H_2O bath. DBU (4.1 mL, 27 mmol) and TBDMSCl (4.2 g, 27 mmol) were added and the reaction mixture was stirred at room temperature for 4 h. H_2O and EtOAc were added, the layers were separated and the aqueous layer was extracted with EtOAc. The organic layers were washed with H_2O and brine, dried with $MgSO_4$ and concentrated by rotary evaporation. The crude product was purified by column chromatography (EtOAc:pentane 1:4) to give **4** (4.6 g, 58%) as yellow solid. ^1H NMR ($CDCl_3$): δ 7.72 (dm, J = 7.9 Hz, 1H), 7.66 (dd, J = 1.6, 7.9 Hz, 1H), 7.38 (dd, J = 7.9, 7.9 Hz, 1H), 3.99 (s, 2H), 3.78–3.73 (m, 2H), 2.77–2.72 (m, 2H), 2.09 (br s, 1H), 0.89 (s, 9), 0.06 (s, 6H). ^{13}C NMR ($CDCl_3$): δ 149.4, 141.4, 132.8, 127.3, 125.7, 123.7, 62.5, 51.3, 51.0, 26.1, 18.5, −5.1. Anal. Calcd for $C_{15}H_{25}ClN_2O_3Si$: C, 52.23; H, 7.31; N, 8.12, found: C, 52.52; H, 7.45; N, 8.18.

4.1.3. (*S*)-2-Amino-*N*-(2-(*tert*-butyldimethylsilyloxy)ethyl)-*N*-(2-chloro-3-nitrobenzyl)-3-(1*H*-indol-3-yl)propanamide (5)

To a solution of **4** (1.0 g, 2.9 mmol) in DCM (25 mL) was added Fmoc-L-Trp-OH (1.5 g, 3.5 mmol), HATU (1.3 g, 3.5 mmol) and DIEA (1.1 mL, 6.4 mmol). The reaction mixture was stirred at room temperature overnight. H_2O and EtOAc were added, the layers were

separated and the aqueous layer was extracted with EtOAc. The organic layers were washed with H_2O and brine, dried with $MgSO_4$, concentrated by rotary evaporation and purified by column chromatography (EtOAc:hexane 1:2). The resulting Fmoc protected amine was dissolved in dry THF (20 mL) and DBU (0.47 mL, 3.1 mmol) and stirred at room temperature for 1.5 h. The crude product was purified by column chromatography (2% MeOH in DCM). Concentration by rotary evaporation gave **5** (1.2 g, 77%) as pale yellow solid. $[\alpha]_D^{23}$ = +54° (*c* = 1.00, DCM). ^{1}H NMR ($CDCl_3$): δ (~5:3 mixture of rotamers) 8.32–8.21 (m, 1H), 7.64–7.58 (m, 2H), 7.40–7.30 (m, 1H), 7.23–6.95 (m, 5H), 4.87 & 4.76 (minor) (d, *J* = 16.4 & 18.6 (minor) Hz, 1H), 4.70 (minor) & 4.57 (d, *J* = 16.4 & 18.6 (minor) Hz, 1H), 4.27–4.22 & 3.68–3.63 (minor) (m, 1H), 3.84–3.36 (m, 3H), 3.17–3.09 (m, 1H), 3.24–3.13 (m, 1H), 3.03 & 2.89 (minor) (dd, *J* = 7.1, 14.1 & 7.6, 14.1 (minor) Hz, 1H), 1.70 (br s, 2H), 0.86 (s, 9H), 0.030–(−0.004) (m, 6H). ^{13}C NMR ($CDCl_3$): δ (~5:3 mixture of rotamers) 176.7 & 176.1 (minor), 149.2 & 149.1 (minor), 138.3 & 138.2 (minor), 136.5 & 136.4 (minor), 131.6 & 129.7 (minor), 127.54 (minor) & 127.20, 127.52 & 127.33 (minor), 125.1 & 124.4 (minor), 124.0 (minor) & 123.6, 123.3 & 123.2 (minor), 122.43 (minor) & 122.39, 119.88 (minor) & 119.86, 118.7 & 118.4 (minor), 111.8 & 111.6 (minor), 111.5 & 111.4 (minor), 61.7 (minor) & 61.6, 52.5 (minor) & 51.8, 50.8 (minor) & 48.1, 50.2 & 49.6 (minor), 32.9 (minor) & 32.4, 26.0 & 25.9 (minor), 18.4 & 18.2 (minor), −5.3 (minor) & −5.4. Anal. Calcd for $C_{26}H_{35}ClN_4O_4Si$: C, 58.80; H, 6.64; N, 10.55, found: C, 59.02; H, 6.75; Cl, 6.67; N, 10.55.

4.1.4. (*S*)-2-((1*H*-Indol-3-yl)methyl)-4-(2-(*tert*-butyldimethylsilyloxy)ethyl)-9-nitro-4,5-dihydro-1*H*-benzo[*e*][1,4]diazepin-3(2*H*)-one (6)

To a solution of **5** (1.2 g, 2.2 mmol) in DMSO (25 mL) was added Et_3N (0.47 mL, 3.4 mmol). The reaction mixture was stirred at 100 °C for 26 h. H_2O and EtOAc were added, the layers were separated and the aqueous layer was extracted with EtOAc. The organic layers were washed with H_2O, brine, dried with $MgSO_4$, concentrated by rotary evaporation and purified by column chromatography (2% MeOH in DCM) to give **6** (0.73 g, 66%) as orange solid. $[\alpha]_D^{23}$ = −149° (*c* = 1.00, DCM). ^{1}H NMR ($CDCl_3$): δ 8.50 (d, *J* = 2.5 Hz, 1H), 8.47–8.41 (m, 1H), 8.00 (dd, *J* = 1.7, 8.7 Hz, 1H), 7.62–7.58 (m, 1H), 7.45–7.38 (m, 1H), 7.35 (d, *J* = 2.5 Hz, 1H), 7.23–7.18 (m, 1H), 7.17–7.11 (m, 1H), 7.06 (dd, *J* = 1.7, 7.1 Hz, 1H), 6.47 (dd, *J* = 7.1, 8.7 Hz, 1H), 5.38 (d, *J* = 16.6 Hz, 1H), 5.27 (ddd, *J* = 2.5, 4.5, 10.0 Hz, 1H), 4.06 (d, *J* = 16.6 Hz, 1H), 3.90–3.74 (m, 3H), 3.60 (ddd, *J* = 1.0, 4.5, 15.1 Hz, 1H), 3.52–3.45 (m, 1H), 3.21 (dd, *J* = 10.0, 15.1 Hz, 1H), 0.91 (s, 9H), 0.058 (s, 3H), 0.056 (s, 3H). ^{13}C NMR ($CDCl_3$): δ 169.3, 144.5, 136.8, 135.9, 132.8, 127.2, 127.0, 124.7, 123.0, 122.3, 119.6, 118.4, 115.2, 111.8, 110.1, 62.0, 54.4, 53.2, 49.8, 27.5, 26.0, 18.3, −5.3.

4.1.5. (*S*)-*tert*-Butyl 3-((4-(2-(*tert*-butyldimethylsilyloxy)ethyl)-9-nitro-3-oxo-2,3,4,5-tetrahydro-1*H*-benzo[*e*][1,4]diazepin-2-yl)methyl)-1*H*-indole-1-carboxylate (7)

The amine **6** (0.56 g, 1.1 mmol) was dissolved in MeCN (35 mL). Boc_2O (0.37 g, 1.7 mmol) and DMAP (0.21 g, 1.7 mmol) were added and the reaction mixture was stirred at room temperature for 2 h. H_2O and DCM were added, the layers were separated and the aqueous layer was extracted with DCM. The organic layers were washed with saturated aqueous $NaHCO_3$, H_2O, 1.0 M aqueous $KHSO_4$ and brine, dried with $MgSO_4$ and concentrated by rotary evaporation. The crude product was purified by column chromatography (0.5% MeOH in DCM) to give **7** (0.52 g, 77%) as yellow solid. $[\alpha]_D^{23}$ = −86° (*c* = 1.03, DCM). ^{1}H NMR ($CDCl_3$): δ 8.46 (d, *J* = 2.9 Hz, 1H), 8.21–8.14 (m, 1H), 8.05 (dd, *J* = 1.7, 8.7 Hz, 1H), 7.69 (s, 1H), 7.59–7.56 (m, 1H), 7.37–7.30 (m, 1H), 7.29–7.23 (m, 1H), 7.10 (dd, *J* = 1.7, 7.1 Hz, 1H), 6.52 (dd, *J* = 7.1, 8.7 Hz, 1H), 5.40 (d, *J* = 16.9 Hz, 1H), 5.21 (ddd, *J* = 2.9, 4.8, 9.2 Hz, 1H), 4.09 8 (d, *J* = 16.9 Hz, 1H), 3.89–3.71 (m, 3H), 3.54 (ddd, *J* = 1.2, 4.8, 15.1 Hz, 1H), 3.52–3.43 (m, 1H), 3.13 (dd, *J* = 9.2, 15.1 Hz, 1H), 1.68 (s, 9H), 0.88 (s, 9H), 0.025 (s, 3H), 0.019 (s, 3H). ^{13}C NMR ($CDCl_3$): δ 168.7, 149.5, 144.0, 135.8, 135.7, 133.1, 129.9, 127.2, 125.2, 124.6, 122.9, 122.6, 118.5, 115.5, 115.3, 115.1, 83.7, 61.9, 54.0, 53.2, 49.7, 28.2, 27.0, 25.9, 18.2, -5.5. Anal. Calcd for $C_{31}H_{42}N_4O_6Si$: C, 62.60; H, 7.12; N, 9.42, found: C, 62.81; H, 7.29; N, 9.26.

4.1.6. (*S*)-*tert*-Butyl 3-((4-(2-hydroxyethyl)-9-nitro-3-oxo-2,3,4,5-tetrahydro-1*H*-benzo[*e*][1,4]diazepin-2-yl)methyl)-1*H*-indole-1-carboxylate (8)

To a solution of **7** (0.48 g, 8.0 mmol) in THF (15 mL) was added 1.0 M TBAF in THF (1.0 mL). After 20 min, H_2O and EtOAc were added, the layers were separated and the aqueous layer was extracted with EtOAc. The organic layers were washed with H_2O, brine, dried with Na_2SO_4 and concentrated by rotary evaporation. The resulting product was purified by column chromatography (2% MeOH in DCM) to give the deprotected alcohol **8** (0.34 g, 89%) as orange solid. $[\alpha]_D^{23}$ = −11° (*c* = 1.00, DCM). ^{1}H NMR ($CDCl_3$): δ 8.45 (d, *J* = 2.9 Hz, 1H), 8.22–8.13 (m, 1H), 8.06 (dd, *J* = 1.6, 8.6 Hz, 1H), 7.70 (s, 1H), 7.59–7.56 (m, 1H), 7.36–7.32 (m, 1H), 7.29–7.24 (m, 1H), 7.13 (dd, *J* = 1.6, 7.1 Hz, 1H), 6.54 (dd, *J* = 7.1, 8.6 Hz, 1H), 5.47 (d, *J* = 16.7 Hz, 1H), 5.23 (ddd, *J* = 2.9, 4.8, 9.0 Hz, 1H), 3.98 (d, *J* = 16.7 Hz, 1H), 3.85–3.71 (m, 3H), 3.68–3.59 (m, 1H), 3.54 (ddd, *J* = 1.1, 4.8, 15.1 Hz, 1H), 3.14 (dd, *J* = 9.0, 15.1 Hz, 1H), 1.88 (br s, 1H), 1.68 (s, 9H). ^{13}C NMR ($CDCl_3$): δ 169.7, 149.5, 143.8, 135.8 (2 signals), 133.2, 129.9, 127.6, 125.3, 124.7, 122.6, 122.5, 118.5, 115.5, 115.4, 114.9, 83.8, 61.8, 54.0, 53.1, 50.4, 28.2, 27.0.

4.1.7. (*S*)-2-(2-((1-(*tert*-Butoxycarbonyl)-1*H*-indol-3-yl)methyl)-9-nitro-3-oxo-2,3-dihydro-1*H*-benzo[*e*][1,4]diazepin-4(5*H*)-yl)acetic acid (9)

DMSO (0.10 mL, 1.4 mmol) was added dropwise to a solution of oxalyl chloride (0.060 mL, 0.70 mmol) in dry DCM (2.0 mL) at −78 °C. After 15 min, a solution of the deprotected alcohol **8** (0.23 g, 0.47 mmol) in dry DCM (3.0 mL), was added dropwise. The reaction mixture was stirred at −78 °C for 1.5 h. Et_3N (0.26 mL, 1.9 mmol) was added and the mixture was allowed to warm to −30 °C over 1 h. H_2O and DCM were added, the layers were separated and the aqueous layer was extracted with DCM. The organic layers were washed with 1.0 M aqueous $KHSO_4$, H_2O, saturated aqueous $NaHCO_3$ and brine, were dried with $MgSO_4$ and concentrated by rotary evaporation. The resulting aldehyde was dissolved in *t*-BuOH (5.0 mL) and cyclohexene (0.92 mL, 9.4 mmol). The solution was cooled on an ice-bath and a cold solution of $NaClO_2$ (0.53 g, 4.7 mmol) and $NaH_2PO_4{\cdot}H_2O$ (0.64 g, 4.7 mmol) in H_2O (2.5 mL) was added. The reaction mixture was stirred for 2.5 h and EtOAc was added, the layers were separated and the aqueous layer was extracted with EtOAc. The organic layer was washed with H_2O, brine, dried with $MgSO_4$ and concentrated by rotary evaporation. The crude product was purified by column chromatography (gradient elution, 2% MeOH in DCM to 10% MeOH in DCM), concentrated and redissolved in EtOAc. The organic solution was washed with 1.0 M aqueous $KHSO_4$, dried with $MgSO_4$ and concentrated by rotary evaporation to give **9** (0.16 g, 69%) as yellow solid. $[\alpha]_D^{23}$ = −95° (*c* = 1.00, DCM). ^{1}H NMR ($CDCl_3$): δ 8.45 (d, *J* = 2.9 Hz, 1H), 8.23–8.12 (m, 1H), 8.06 (dd, *J* = 1.7, 8.8 Hz, 1H), 7.70 (s, 1H), 7.61–7.56 (m, 1H), 7.38–7.31 (m, 1H), 7.30–7.24 (m, 1H), 7.14–7.07 (m, 1H), 7.10 (dd, *J* = 1.7, 7.1 Hz, 1H), 6.55 (dd, *J* = 7.1, 8.8 Hz, 1H), 5.54 (d, *J* = 16.9 Hz, 1H), 5.26 (ddd, *J* = 2.9, 4.5, 9.2 Hz, 1H), 4.66 (d, *J* = 17.6 Hz, 1H), 4.04 (d, *J* = 17.6 Hz, 1H), 3.87 (d, *J* = 16.9 Hz, 1H), 3.55 (ddd, *J* = 1.0, 4.5, 15.2 Hz, 1H), 3.15 (dd, *J* = 9.2, 15.2 Hz, 1H), 1.68 (s, 9H). ^{13}C NMR ($CDCl_3$): δ 172.5, 169.8, 149.5, 143.7, 135.8 (2 signals), 133.4, 129.8, 127.5, 125.3, 124.7, 122.6, 121.8, 118.6, 115.54, 115.50, 114.7, 83.9, 53.7, 52.9, 48.2, 28.2, 26.9. Anal. Calcd for $C_{25}H_{26}N_4O_7$: C, 60.72; H, 5.30; N, 11.33, found: C, 60.84; H, 5.46; N, 11.19.

4.1.8. (*S*)-2-(9-(((9*H*-Fluoren-9-yl)methoxy)carbonylamino)-2-((1-(*tert*-butoxycarbonyl)-1*H*-indol-3-yl)methyl)-3-oxo-2,3-dihydro-1*H*-benzo[*e*][1,4]diazepin-4(5*H*)-yl)acetic acid (10)

To a solution of **9** (0.10 g, 0.20 mmol) in MeOH (10 mL) was added Pd/C 10% (0.015 g, 0.014 mmol). The reaction mixture was stirred under H_2 atmosphere for 4 h. The catalyst was filtered off and the solvent was removed by rotary evaporation. The crude product was dissolved in 1,4-dioxane (7.0 mL) and was cooled to 0 °C. FmocCl (0.10 g, 0.40 mmol) was added followed by a solution of Na_2CO_3 (0.085 g, 8.0 mmol) in H_2O (2.0 mL). The reaction mixture was stirred at room temperature over night and then washed with ether. The aqueous layer was acidified to pH 3 by addition of 5% aqueous citric acid and was extracted with EtOAc. The organic layers were washed with H_2O, brine, dried with $MgSO_4$ and concentrated by rotary evaporation to give **10** (0.11 g, 79%) as beige foam. $[\alpha]_D^{23} = -50°$ (*c* = 1.01, DCM). ^{1}H NMR (DMSO-d_6, 70° C): δ 8.40 (br s, 1H), 7.98 (dm, *J* = 8.3 Hz, 1H), 7.86 (dm, *J* = 7.7 Hz, 2H), 7.64 (dm, *J* = 7.9 Hz, 1H), 7.64–7.58 (m, 2H), 7.58 (s, 1H), 7.42–7.36 (m, 2H), 7.31–7.23 (m, 3H), 7.21–7.16 (m, 1H), 7.04 (dm, *J* = 7.6 Hz, 1H), 6.88 (dd, *J* = 1.6, 7.6 Hz, 1H), 6.57 (dd, *J* = 7.6, 7.6 Hz, 1H), 5.44 (d, *J* = 16.5 Hz, 1H), 4.99 (dd, *J* = 5.6, 7.6 Hz, 1H), 4.93–4.71 (m, 1H), 4.34 (d, *J* = 17.1 Hz, 1H), 4.27–4.22 (m, 2H), 4.19–4.14 (m, 1H), 4.07 (d, *J* = 16.5 Hz, 1H), 3.93 (d, *J* = 17.1 Hz, 1H), 3.29 (dd, *J* = 5.6, 15.3 Hz, 1H), 3.00 (dd, *J* = 7.6, 15.3 Hz, 1H), 1.57 (s, 9H).

4.2. Solid phase peptide synthesis (SPPS)

Pseudopeptides **11**–**15** were prepared manually in a disposable syringe equipped with a porous polyethylene filter using standard SPPS Fmoc/*t*-Bu chemistry. The Fmoc group was removed by treatment with 20% piperidine in DMF for 10 + 10 min. Couplings were performed in DMF, using PyBOP in the presence of DIEA. Amino acids with the following side chain protection were used: Asp(O*t*-Bu), Glu(O*t*-Bu), Trp(Boc). The crude pseudopeptides were purified by preparative RP-HPLC.

4.2.1. Ac-Glu-Asp-Asp-I-Phe (11)

Compound **10** (0.10 g, 0.15 mmol), PyBOP (0.12 mg, 0.23 mmol) and DIEA (0.052 mL, 0.30 mmol) were dissolved in DMF (1.5 mL). The mixture was added to *H*-L-Phe-2-chlorotrityl resin (0.18 g, 0.15 mmol) in a 2 mL syringe vessel and allowed to react for 22 h. The resin was washed with DMF and the Fmoc group was removed. After washing with DMF, DCM and MeOH the resin was dried in vacuo to give 0.22 g. The material was further reacted in DMF (1.0 mL) with Fmoc-L-Asp(O*t*Bu)-OH (0.19 g, 0.45 mmol) and PyBOP (0.23 g, 0.45 mmol) in the presence of DIEA (0.16 mL, 0.90 mmol) for 24 h. The resin was washed and the coupling was repeated. Thereafter, the resin was washed and deprotected. After washing with DMF, DCM and MeOH the resin was dried in vacuo to give 0.23 g.

Two thirds of the material (0.15 g, 0.10 mmol) was transferred to another syringe and reacted in DMF (1.0 mL) with Fmoc-L-Asp(O*t*Bu)-OH (0.17 g, 0.40 mmol) and PyBOP (0.21 g, 0.40 mmol) in the presence of DIEA (0.14 mL, 0.80 mmol) for 17 h. The resin was washed and deprotected. After washing with DMF, DCM and MeOH the resin was dried in vacuo to give 0.16 g.

Half of the remaining material (0.80 g, 0.050 mmol) was transferred to another syringe and reacted in DMF (1.0 mL) with Fmoc-L-Glu(O*t*Bu)-OH (0.085 g, 0.20 mmol) and PyBOP (0.10 g, 0.20 mmol) in the presence of DIEA (0.070 mL, 0.40 mmol) for 47 h. The resin was washed and deprotected. After washing with DMF, DCM and MeOH the resin was dried in vacuo to give 0.084 g.

The material was then reacted in DMF (1.0 mL) with acetic anhydride (0.048 mL, 0.50 mmol) in the presence of DIEA (0.087 mL, 0.50 mmol) for 1 h. After washing with DMF, 20% piperidine in DMF, DMF, DCM and MeOH the resin was dried in vacuo to give 0.084 g. The pseudopeptide polymer was treated with triethylsilane (0.075 mL) and 95% aqueous TFA (1.5 mL) for 1.5 h. The polymer was removed by filtration and washed with TFA (2 × 0.3 mL). The combined filtrates were evaporated in a stream of nitrogen to approximately 0.1 mL and the product was precipitated with diethyl ether (12 mL). It was collected by centrifugation and washed with more diethyl ether (3 × 4 mL) and dried in vacuo to give 0.034 g. The crude product was purified by preparative RP-HPLC. Selected fractions were pooled and lyophilized to give pseudopeptide **11** (0.021 g, 45%). ^{1}H NMR (CD_3OD): δ 7.65 (dm, *J* = 7.9 Hz, 1H), 7.34 (dm, *J* = 7.9 Hz, 1H), 7.30 (s, 1H), 7.24–7.10 (m, 5H), 7.09–7.04 (m, 1H), 7.04–6.99 (m, 1H), 6.96 (dd, *J* = 1.3, 7.6 Hz, 1H), 6.80 (dd, *J* = 1.3, 7.6 Hz, 1H), 6.54 (dd, *J* = 7.6, 7.6 Hz, 1H), 5.17 (d, *J* = 16.8 Hz, 1H), 4.99 (dd, *J* = 5.7, 7.9 Hz, 1H), 4.75 (dd, *J* = 6.7, 6.7 Hz, 1H), 4.65 (dd, *J* = 6.0, 6.5 Hz, 1H), 4.56 (d, *J* = 16.3 Hz, 1H), 4.54 (dd, *J* = 5.7, 8.2 Hz, 1H), 4.30–4.24 (m, 1H), 3.70 (d, *J* = 16.8 Hz, 1H), 3.64 (d, *J* = 16.3 Hz, 1H), 3.43 (dd, *J* = 5.7, 14.9 Hz, 1H), 3.24 (dd, *J* = 4.7, 14.7 Hz, 1H), 3.09 (dd, *J* = 7.9, 14.9 Hz, 1H), 2.91 (dd, *J* = 8.2, 14.7 Hz, 1H), 2.82–2.73 (m, 3H), 2.67 (dd, *J* = 6.0, 16.1 Hz, 1H), 2.41–2.33 (m, 2H), 2.12–2.00 (m, 1H), 1.98 (s, 3H), 1.98–1.88 (m, 1H). HRMS calcd for $C_{44}H_{49}N_8O_{14}$ ($M+H^+$): 913.3368, found: 913.3378. RP-HPLC purity (column 1: 96%, column 2: 96%).

4.2.2. Ac-Glu-Asp-Asp-Asp-I-Phe (12)

A solution of Fmoc-L-Asp(O*t*Bu)-OH (0.082 g, 0.20 mmol), PyBOP (0.10 g, 0.20 mmol) and DIEA (0.070 mL, 0.40 mmol) in DMF (1.0 mL) was added to *H*-Asp(O*t*Bu)-Asp(O*t*Bu)-I-Phe-2-chlorotrityl resin (0.083 g, 0.050 mmol) in a 2 mL syringe vessel and was reacted for 4 h. The resin was washed and deprotected. After washing with DMF, a solution of Fmoc-L-Glu(O*t*Bu)-OH (0.085 g, 0.20 mmol), PyBOP (0.10 g, 0.20 mmol) and DIEA (0.070 mL, 0.40 mmol) in DMF (1.0 mL) was added and allowed to react for 19 h. The resin was washed and deprotected. After washing with DMF, DCM and MeOH the resin was dried in vacuo to give 0.093 g. Then, the material was reacted in DMF (1.0 mL) with acetic anhydride (0.048 mL, 0.50 mmol) in the presence of DIEA (0.087 mL, 0.50 mmol) for 1 h. After washing with DMF, DCM and MeOH the resin was dried in vacuo to give 0.094 g. Cleavage from the resin and isolation of crude **12** (0.037 g) was performed as described above for **11**. Purification by preparative RP-HPLC gave pseudopeptide **12** (0.012 g, 23%). ^{1}H NMR (CD_3OD): δ 7.65 (dm, *J* = 7.8 Hz, 1H), 7.35 (dm, *J* = 8.0 Hz, 1H), 7.31 (s, 1H), 7.23–7.11 (m, 5H), 7.09–7.04 (m, 1H), 7.04–6.98 (m, 1H), 6.95 (dm, *J* = 7.7 Hz, 1H), 6.79 (dm, *J* = 7.7 Hz, 1H), 6.54 (dd, *J* = 7.7, 7.7 Hz, 1H), 5.17 (d, *J* = 16.9 Hz, 1H), 4.99 (dd, *J* = 5.5, 7.5 Hz, 1H), 4.73 (dd, *J* = 6.7, 6.7 Hz, 1H), 4.66–4.60 (m, 2H), 4.59 (d, *J* = 16.1 Hz, 1H), 4.57 (dd, *J* = 4.7, 8.2 Hz, 1H), 4.30 (dd, *J* = 5.6, 7.9 Hz, 1H), 3.71 (d, *J* = 16.9 Hz, 1H), 3.64 (d, *J* = 16.1 Hz, 1H), 3.44 (dd, *J* = 5.5, 14.8 Hz, 1H), 3.24 (dd, *J* = 4.7, 13.9 Hz, 1H), 3.11 (dd, *J* = 7.5, 14.8 Hz, 1H), 2.92 (d, *J* = 8.2, 13.9 Hz, 1H), 2.88–2.77 (m, 4H), 2.77–2.67 (m, 2H), 2.38–2.32 (M, 2H), 2.12–2.02 (m, 1H), 2.00–1.89 (m, 1H), 1.96 (s, 3H). HRMS calcd for $C_{48}H_{54}N_9O_{17}$ ($M+H^+$): 1028.3638, found: 1028.3627. RP-HPLC purity (column 1: 97%, column 2: 96%).

4.2.3. Ac-Asp-I-Phe (13)

Acetic anhydride (0.048 mL, 0.50 mmol) and DIEA (0.087 mL, 0.50 mmol) in DMF (1.0 mL) were added to *H*-Asp(O*t*Bu)-I-Phe-2-chlorotrityl resin (0.076 g, 0.050 mmol) and was reacted in a 2 mL syringe vessel for 1 h. The resin was washed with DMF, DCM and MeOH and was dried in vacuo to give 0.078 g. Cleavage from the resin and isolation of crude **13** (0.025 g) was performed as described above for **11**. Purification by preparative RP-HPLC gave pseudopeptide 13 (0.0076 g, 23%). ^{1}H NMR (CD_3OD): δ 7.65 (dm, *J* = 7.8 Hz, 1H), 7.33 (dm, *J* = 8.0 Hz, 1H), 7.27 (s, 1H),

7.23–7.11 (m, 5H), 7.08 (ddd, J = 1.4, 7.1, 8.0 Hz, 1H), 7.02 (ddd, J = 1.3, 7.1, 7.8 Hz, 1H), 6.99 (dd, J = 1.6, 7.6 Hz, 1H), 6.81 (dd, J = 1.6, 7.6 Hz, 1H), 6.57 (dd, J = 7.6, 7.6 Hz, 1H), 5.20 (d, J = 16.6 Hz, 1H), 5.00 (dd, J = 6.0, 7.1 Hz, 1H), 4.74 (dd, J = 6.6, 6.8 Hz, 1H), 4.59 (dd, J = 5.1, 8.5 Hz, 1H), 4.55 (d, J = 16.3 Hz, 1H), 3.74 (d, J = 16.6 Hz, 1H), 3.67 (d, J = 16.3 Hz, 1H), 3.45 (dd, J = 6.0, 15.1 Hz, 1H), 3.22 (dd, J = 5.1, 14.0 Hz, 1H), 3.14 (dd, J = 7.1, 15.1 Hz, 1H), 2.90 (dd, J = 6.8, 17.0 Hz, 1H), 2.72 (dd, J = 6.6, 17.0 Hz, 1H), 1.94 (s, 3H). HRMS calcd for $C_{35}H_{37}N_6O_8$ ($M+H^+$): 669.2673, found: 669.2678. RP-HPLC purity (column 1: 96%, column 2: 96%).

4.2.4. Fmoc-Asp-I-Phe (14)

Compound **10** (0.035 g, 0.051 mmol), PyBOP (0.027 mg, 0.051 mmol) and DIEA (0.018 mL, 0.10 mmol) were dissolved in DMF (1.5 mL). The mixture was added to *H*-L-Phe-2-chlorotrityl resin (0.057 g, 0.049 mmol) in a 2 mL syringe vessel and allowed to react for 24 h. After washing with DMF, DCM and MeOH the resin was dried in vacuo to give 0.087 g.

Part of the material (0.044 g, 0.025 mmol) was transferred to another syringe and the resin deprotected. After washing with DMF, a solution of Fmoc-L-Asp(O*t*Bu)-OH (0.041 g, 0.10 mmol), PyBOP (0.052 g, 0.10 mmol) and DIEA (0.035 mL, 0.20 mmol) in DMF (1.0 mL) was added and allowed to react for 22 h. After washing with DMF, DCM and MeOH the resin was dried in vacuo to give 0.047 g. Cleavage from the resin and isolation of crude **14** (0.013 g) was performed as described above for **11**. Purification by preparative RP-HPLC gave pseudopeptide **14** (0.0028 g, 14%). ^{1}H NMR (CD_3OD): δ 7.77–7.72 (m, 2H), 7.62 (dm, J = 7.9 Hz, 1H), 7.57 (dm, J = 7.8 Hz, 1H), 7.52–7.48 (m, 1H), 7.36–7.28 (m, 3H), 7.24–7.11 (m, 8H), 7.08–7.03 (m, 1H), 7.00–6.95 (m, 2H), 6.81 (dd, J = 1.6, 7.7 Hz, 1H), 6.58 (dd, J = 7.7, 7.7 Hz, 1H), 5.23 (dm, J = 16.5 Hz, 1H), 5.04–4.99 (m, 1H), 4.66 (dd, J = 5.1, 9.0 Hz, 1H), 4.53 (d, J = 16.4 Hz, 1H), 4.53–4.48 (m, 1H), 4.42–4.31 (m, 2H), 4.17–4.12 (m, 1H), 3.73 (dm, J = 16.5 Hz, 1H), 3.71 (dd, J = 16.4 Hz, 1H), 3.48 (dd, J = 15.0, 6.2 Hz, 1H), 3.22–3.15 (m, 2H), 2.91–2.82 (m, 2H), 2.70 (dd, J = 16.5, 6.9 Hz, 1H). HRMS calcd for $C_{48}H_{45}N_6O_9$ ($M+H^+$): 849.3248, found: 849.3242. RP-HPLC purity (column 1: >99%, column 2: >99%).

4.2.5. (*S*)-2-(2-((1*H*-Indol-3-yl)methyl)-9-(((9*H*-fluoren-9-yl)methoxy)carbonylamino)-3-oxo-2,3-dihydro-1*H*-benzo[*e*][1,4]diazepin-4(5*H*)-yl)acetic acid (15)

To a solution of **10** (0.0080 g, 0.012 mmol) in DCM (0.50 mL) was added TFA (0.50 mL) at 0 °C. The reaction mixture was stirred for 1.5 h at room temperature. More DCM was added and the solvent was evaporated. The residue was dissolved in MeCN and H_2O and was lyophilized. The crude product was purified by preparative RP-HPLC (MeCN/H_2O gradient with 0.1% TFA) to give **15** (0.0031 g, 44%) as white solid. ^{1}H NMR (DMSO-d_6, 70 °C): δ 10.66 (br s, 1H), 8.41 (br s, 1H), 7.87 (dm, J = 7.3 Hz, 2H), 7.66 (dm, J = 7.4 Hz, 2H), 7.59 (dm, J = 7.8 Hz, 1H), 7.44–7.38 (m, 2H), 7.35–7.27 (m, 3H), 7.19 (d, J = 2.5 Hz, 1H), 7.04–6.96 (m, 2H), 6.96–6.90 (m, 1H), 6.84 (dm, J = 7.7 Hz, 1H), 6.52 (dd, J = 7.7, 7.7 Hz, 1H), 5.36 (d, J = 16.7 Hz, 1H), 4.93–4.86 (m, 1H), 4.73 (d, J = 4.7 Hz, 1H), 4.31 (d, J = 16.6 Hz, 1H), 4.31–4.25 (m, 2H), 4.22–4.16 (m, 1H), 4.01 (d, J = 16.7 Hz, 1H), 3.68 (d, J = 16.6 Hz, 1H), 3.33 (dd, J = 5.5, 14.9 Hz, 1H), 2.98 (dd, J = 7.6, 14.9 Hz, 1H). HRMS calcd for $C_{35}H_{31}N_4O_5$ ($M+H^+$): 587.2294, found: 587.2288. RP-HPLC purity (column 1: >99%, column 2: >99%).

4.2.6. (*S*)-*tert*-Butyl 3-((9-(((9*H*-fluoren-9-yl)methoxy)carbonylamino)-4-(2-(*tert*-butyldimethylsilyloxy)ethyl)-3-oxo-2,3,4,5-tetrahydro-1*H*-benzo[*e*][1,4]diazepin-2-yl)methyl)-1*H*-indole-1-carboxylate (16)

To a solution of **7** (0.040 g, 0.067 mmol) in EtOH (15 mL) was added Pd/C 10% (10 mg, 0.0091 mmol). The reaction mixture was stirred under H_2 atmosphere for 2 h. The catalyst was filtered off and the solvent was removed by rotary evaporation. The resulting amine was dissolved in 1,4-dioxane (3.0 mL) and was cooled to 0 °C. FmocCl (0.035 g, 0.13 mmol) was added followed by a solution of Na_2CO_3 (0.028 g, 0.27 mmol) in H_2O (1.0 mL). The reaction mixture was stirred at room temperature for 1.5 h and then diethyl ether was added. The organic layer was separated and was concentrated by rotary evaporation. The residue was dissolved in DCM and was washed with 1.0 M aqueous $KHSO_4$, H_2O, and brine. The crude product was purified by column chromatography (0.5% MeOH in DCM) and was concentrated by rotary evaporation to give **16** (0.033 g, 62%) as beige foam. $[\alpha]_D^{23} = -62°$ (c = 1.00, DCM). ^{1}H NMR (DMSO-d_6): δ 8.62 (br s, 1H), 7.97 (dm, J = 8.4 Hz, 2H), 7.89 (dm, J = 7.7 Hz, 2H), 7.69 (dm, J = 7.8 Hz, 1H), 7.71–7.61 (m, 2H), 7.58 (s, 1H), 7.43–7.37 (m, 2H), 7.31–7.23 (m, 3H), 7.11–6.96 (m, 1H), 6.86 (dd, J = 1.6, 7.7 Hz, 1H), 6.55 (dd, J = 7.7, 7.7 Hz, 1H), 5.44 (d, J = 16.6 Hz, 1H), 5.04–5.98 (m, 1H), 4.94–4.85 (m, 1H), 4.34–4.12 (m, 3H), 4.02 (d, J = 16.6 Hz, 1H), 3.68–3.57 (m, 3H), 3.31–3.26 (m, 1H), 3.27 (dd, J = 6.7, 14.8 Hz, 1H), 2.95 (dd, J = 7.0, 14.8 Hz, 1H) 1.55 (s, 9H), 0.81 (s, 9H), -0.052 (s, 6H). Anal. Calcd for $C_{46}H_{54}N_4O_6Si\cdot 1H_2O$: C, 68.62; H, 7.01; N, 6.96, found: C, 68.67; H, 6.99; N, 6.84.

4.2.7. (*S*)-(9*H*-Fluoren-9-yl)methyl 2-((1*H*-indol-3-yl)methyl)-4-(2-hydroxyethyl)-3-oxo-2,3,4,5-tetrahydro-1*H*-benzo[*e*][1,4]diazepin-9-ylcarbamate (17)

To a solution of **16** (0.033 g, 0.042 mmol) in DCM (1.0 mL) was added TFA (0.50 mL) at 0 °C. The reaction mixture was stirred for 1.5 h at room temperature. More DCM was added and the solvent was evaporated. The residue was dissolved in MeCN and H_2O and was lyophilized. The crude product was purified by preparative RP-HPLC (MeCN/H_2O gradient with 0.1% TFA) to give **17** (0.017 g, 71%) as white solid. ^{1}H NMR (DMSO-d_6, 70 °C): δ 10.66 (br s, 1H), 8.43 (br s, 1H), 7.87 (dm, J = 7.7 Hz, 2H), 7.66 (dm, J = 7.6 Hz, 2H), 7.60 (dm, J = 7.8 Hz, 1H), 7.44–7.38 (m, 2H), 7.34–7.28 (m, 3H), 7.19 (d, J = 2.5 Hz, 1H), 7.04–6.91 (m, 3H), 6.87 (dd, J = 1.6, 7.7 Hz, 1H), 6.52 (dd, J = 7.7, 7.7 Hz, 1H), 5.36 (d, J = 16.6 Hz, 1H), 4.90 (dd, J = 6.0, 7.8 Hz, 1H), 4.81–4.62 (m, 1H), 4.31–4.26 (m, 2H), 4.23–4.17 (m, 1H), 4.03 (d, J = 16.6 Hz, 1H), 3.61 (ddd, J = 5.5, 6.6, 12.1 Hz, 1H), 3.49–3.44 (m, 2H), 3.40–3.34 (m, 1H), 3.33 (dd, J = 6.0, 14.8 Hz, 1H), 2.98 (dd, J = 7.8, 14.8 Hz, 1H). HRMS calcd for $C_{35}H_{33}N_4O_4$ ($M+H^+$): 573.2502, found: 573.2498. RP-HPLC purity (column 1: >99%, column 2: 97%).

4.3. Conformational analysis and molecular modeling

Conformational analysis was performed on the model compound **11m**. The OLPS_2005 force field[22] and the General Born Solvent Accessible (GB/SA) surface area method for water developed by Still et al.,[23] as implemented in the program MacroModel 9.7,[24] was used in the calculation. The conformational search was conducted using the Monte Carlo Multiple Minimum (MCMM)[25] method (50,000 steps) in the batchmin program with default settings. Truncated Newton Conjugate Gradient[26] (TNCG) minimization with a maximum of 5000 iterations was used in the conformational search, with derivative convergence set to 0.05 kJ/mol/Å. Conformations within 5 kcal/mol of the lowest energy minimum were kept. A subsequent reminimization of all conformations was thereafter performed using a maximum of 5000 iterations of PR Conjugate Gradient (PRCG), with the convergence criteria increased to 0.001 kJ/mol/Å. Figure 2 was made in Sybyl-x 2.0 (Tripos International, 1699 South Hanley Rd., St. Louis, MO 63144, USA).

To investigate if model compounds **11m** can adopt similar conformations as the R2 C-terminal fragment from the X-ray structure of *S. typhimurium* RNR, we used shape screening in Phase (v3.1). The R1/R2 holocomplex from *S. typhimurium* was used for these studies (PDB ID: 2BQ1).[11] The structure was pre-processed using

the Protein Preparation Wizard in Maestro, v8.5 (Schroödinger, LLC, New York, NY). The PDB structure contains two R1/R2 dimers and the R1/R2 complex where the last 11 residues of the R2 subunit was present, was used in the modeling (the other R1/R2 complex was deleted). The Ac-Asp-Trp-Asn-Phe fragment from the R2 C-terminus was extracted and the resulting model compound **1m** was used as template in the shape screening. In the volume scoring all atoms were treated the same.

4.4. Fluorescence polarization measurements

The target compounds were evaluated using a competitive fluorescence polarization assay as previously described.[14] All compounds were dissolved in 100% DMSO to a stock concentration of 5–25 mM and stored at −20 °C. A peptide probe with the sequence Dansyl-Gly-Ser-Gly-Glu-Asp-Asp-Asp-Trp-Asp-Phe was used to evaluate the compounds in a competitive binding model as described by Roehrl et al.[27,28] Measurements were done on triplicate reactions on a Perkin Elmer Envision 2104 Multilabel Reader using 340 and 535 nm filters for excitation and emission, respectively.

4.5. RNR activity [^{3}H]CDP assay for IC_{50} determination

The *M. tuberculosis* RNR inhibitory properties of compounds **1**, **12**, **15** and **17** were evaluated in a [^{3}H]CDP assay[29] which was performed as reported by Nurbo et al.[8] The R1 concentration was 1 μM and the R2 concentration 0.5 μM, and the buffer composition was 40 mM Hepes pH 7.5, 6 mM $MgSO_4$, 6 mM NaF, 5 mM DTT, 3 mM ATP, 10 mM CDP, and 3 mM [^{3}H]CDP (888 GBq/mmol). Due to solubility limitations of the inhibitors experiments were restricted to the interval 5–50 μM. The compounds were ranked based on concentration of the compound which caused 50% reduction of the cpm signal at the given conditions. The IC_{50} values are an average of three separate experiments with the standard deviation.

Acknowledgments

We thank Dr. Aleh Yahorau, Department of Pharmaceutical Biosciences, Uppsala University, for conducting HRMS analyses. We also acknowledge the Swedish Foundation for Strategic Research (SSF), the Swedish Research Council (VR) and the EU Sixth Framework Program NM4TB CT:018 923 for financial support.

Supplementary data

Supplementary data associated with this article can be found, in the online version, at http://dx.doi.org/10.1016/j.bmc.2013.01.020.

References and notes

1. In *World Health Organization Global Tuberculosis Control*, 2011. Available at http://www.who.int/tb/publications/global_report/en/, (accessed 16 September 2012).
2. In *Multidrug and Extensively Drug-Resistant TB* (*M/XDR-TB*): *Global Report on Surveillance and Response*, 2010. Available at http://www.who.int/tb/publications/2010/9789245991 91/en/index.html (accessed 16 September 2012).
3. Raviglione, M. C.; Smith, I. M. *N. Eng. J. Med.* **2007**, *356*, 656.
4. Dawes, S. S.; Warner, D. F.; Tsenova, L.; Timm, J.; McKinney, J. D.; Kaplan, G.; Rubin, H.; Mizrahi, V. *Infect. Immun.* **2003**, *71*, 6124.
5. Mowa, M. B.; Warner, D. F.; Kaplan, G.; Kana, B. D.; Mizrahi, V. *J. Bacteriol.* **2009**, *191*, 985.
6. Reichard, P. *Science* **1993**, *260*, 1773.
7. Yang, F.; Curran, S. C.; Li, L.-S.; Avarbock, D.; Graf, J. D.; Chua, M.-M.; Lu, G.; Salem, J.; Rubin, H. *J. Bacteriol.* **1997**, *179*, 6408.
8. Nurbo, J.; Roos, A. K.; Muthas, D.; Wahlstrom, E.; Ericsson, D. J.; Lundstedt, T.; Unge, T.; Karlen, A. *J. Pept. Sci.* **2007**, *13*, 822.
9. Cole, S. T.; Brosch, R.; Parkhill, J.; Garnier, T.; Churcher, C.; Harris, D.; Gordon, S. V.; Eiglmeier, K.; Gas, S.; Barry, C. E.; Tekaia, F.; Badcock, K.; Basham, D.; Brown, D.; Chillingworth, T.; Connor, R.; Davies, R.; Devlin, K.; Feltwell, T.; Gentles, S.; Hamlin, N.; Holroyd, S.; Hornby, T.; Jagels, K.; Krogh, A.; McLean, J.; Moule, S.; Murphy, L.; Oliver, K.; Osborne, J.; Quail, M. A.; Rajandream, M. A.; Rogers, J.; Rutter, S.; Seeger, K.; Skelton, J.; Squares, R.; Squares, S.; Sulston, J. E.; Taylor, K.; Whitehead, S.; Barrell, B. G. *Nature* **1998**, *393*, 537.
10. Sassetti, C. M.; Boyd, D. H.; Rubin, E. J. *Mol. Microbiol.* **2003**, *48*, 77.
11. Uppsten, M.; Farnegardh, M.; Domkin, V.; Uhlin, U. *J. Mol. Biol.* **2006**, *359*, 365.
12. Gao, Y.; Liehr, S.; Cooperman, B. S. *Bioorg. Med. Chem. Lett.* **2002**, *12*, 513.
13. Tan, C. H.; Gao, Y.; Kaur, J.; Cooperman, B. S. *Bioorg. Med. Chem. Lett.* **2004**, *14*, 5301.
14. Ericsson, D. J.; Nurbo, J.; Muthas, D.; Hertzberg, K.; Lindeberg, G.; Karlén, A.; Unge, T. *J. Pept. Sci.* **2010**, *16*, 159.
15. Fuertes, M. J.; Kaur, J.; Deb, P.; Cooperman, B. S.; Smith, A. B. *Bioorg. Med. Chem. Lett.* **2005**, *15*, 5146.
16. Smith, A. B.; Sasho, S.; Barwis, B. A.; Sprengeler, P.; Barbosa, J.; Hirschmann, R.; Cooperman, B. S. *Bioorg. Med. Chem. Lett.* **1998**, *8*, 3133.
17. Dziadulewicz, E. K.; Brown, M. C.; Dunstan, A. R.; Lee, W.; Said, N. B.; Garratt, P. J. *Bioorg. Med. Chem. Lett.* **1999**, *9*, 463.
18. Lauffer, D. J.; Mullican, M. D. *Bioorg. Med. Chem. Lett.* **2002**, *12*, 1225.
19. Lee, J. Y.; Im, I.; Webb, T. R.; McGrath, D.; Song, M. R.; Kim, Y. C. *Bioorg. Chem.* **2009**, *37*, 90.
20. Ripka, W. C.; Delucca, G. V.; Bach, A. C.; Pottorf, R. S.; Blaney, J. M. *Tetrahedron* **1993**, *49*, 3609.
21. Rosenstrom, U.; Skold, C.; Plouffe, B.; Beaudry, H.; Lindeberg, G.; Botros, M.; Nyberg, F.; Wolf, G.; Karlen, A.; Gallo-Payet, N.; Hallberg, A. *J. Med. Chem.* **2005**, *48*, 4009.
22. Kaminski, G. A.; Friesner, R. A.; Tirado-Rives, J.; Jorgensen, W. L. *J. Phys. Chem. B* **2001**, *105*, 6474.
23. Still, W. C.; Tempczyk, A.; Hawley, R. C.; Hendrickson, T. *J. Am. Chem. Soc.* **1990**, *112*, 6127.
24. Mohamadi, F.; Richards, N. G. J.; Guida, W. C.; Liskamp, R.; Lipton, M.; Caufield, C.; Chang, G.; Hendrickson, T.; Still, W. C. *J. Comput. Chem.* **1990**, *11*, 440.
25. Chang, G.; Guida, W. C.; Still, W. C. *J. Am. Chem. Soc.* **1989**, *111*, 4379.
26. Ponder, J. W.; Richards, F. M. *J. Comput. Chem.* **1987**, *8*, 1016.
27. Roehrl, M. H. A.; Kang, S. H.; Aramburu, J.; Wagner, G.; Rao, A.; Hogan, P. G. *Proc. Natl. Acad. Sci. U.S.A.* **2004**, *101*, 7554.
28. Roehrl, M. H. A.; Wang, J. Y.; Wagner, G. *Biochemistry* **2004**, *43*, 16056.
29. Engstrom, Y.; Eriksson, S.; Thelander, L.; Akerman, M. *Biochemistry* **1979**, *18*, 2941.